

1

AD-A222 804

INTERACTION OF ELECTROMAGNETIC
SIGNALS WITH PARTICULATE
CLOUDS

DTIC
ELECTE
JUN 18 1990
S D
to D

APPROVED:

Supervisor: Thomas A. Griffy

Thomas A. Griffy

Dennis E. Wilson

Dennis E. Wilson

DISTRIBUTION STATEMENT A
Approved for public release:
Distribution Unlimited

90 06 15 064

REPORT DOCUMENTATION PAGE

Form Approved
OMB No. 0704-0188

1a. REPORT SECURITY CLASSIFICATION UNCLASSIFIED		1b. RESTRICTIVE MARKINGS NONE	
2a. SECURITY CLASSIFICATION AUTHORITY		3. DISTRIBUTION/AVAILABILITY OF REPORT APPROVED FOR PUBLIC RELEASE; DISTRIBUTION UNLIMITED.	
2b. DECLASSIFICATION/DOWNGRADING SCHEDULE		4. PERFORMING ORGANIZATION REPORT NUMBER(S)	
4. PERFORMING ORGANIZATION REPORT NUMBER(S)		5. MONITORING ORGANIZATION REPORT NUMBER(S) AFIT/CI/CIA-90-030	
6a. NAME OF PERFORMING ORGANIZATION AFIT STUDENT AT University of Texas - Austin	6b. OFFICE SYMBOL <i>(if applicable)</i>	7a. NAME OF MONITORING ORGANIZATION AFIT/CIA	
6c. ADDRESS (City, State, and ZIP Code)		7b. ADDRESS (City, State, and ZIP Code) Wright-Patterson AFB OH 45433-6583	
8a. NAME OF FUNDING / SPONSORING ORGANIZATION	8b. OFFICE SYMBOL <i>(if applicable)</i>	9. PROCUREMENT INSTRUMENT IDENTIFICATION NUMBER	
8c. ADDRESS (City, State, and ZIP Code)		10. SOURCE OF FUNDING NUMBERS	
		PROGRAM ELEMENT NO.	PROJECT NO.
		TASK NO.	WORK UNIT ACCESSION NO.
11. TITLE (Include Security Classification) (UNCLASSIFIED) Interaction of Electromagnetic Signals with Particulate Clouds			
12. PERSONAL AUTHOR(S) Jose Mario Pauda			
13a. TYPE OF REPORT THESIS/DISSERTATION	13b. TIME COVERED FROM _____ TO _____	14. DATE OF REPORT (Year, Month, Day) 1990	15. PAGE COUNT 78
16. SUPPLEMENTARY NOTATION APPROVED FOR PUBLIC RELEASE IAW AFR 190-1 ERNEST A. HAYGOOD, 1st Lt, USAF Executive Officer, Civilian Institution Programs			
17. COSATI CODES		18. SUBJECT TERMS (Continue on reverse if necessary and identify by block number)	
FIELD	GROUP	SUB-GROUP	
19. ABSTRACT (Continue on reverse if necessary and identify by block number)			
20. DISTRIBUTION/AVAILABILITY OF ABSTRACT <input checked="" type="checkbox"/> UNCLASSIFIED/UNLIMITED <input type="checkbox"/> SAME AS RPT. <input type="checkbox"/> DTIC USERS		21. ABSTRACT SECURITY CLASSIFICATION UNCLASSIFIED	
22a. NAME OF RESPONSIBLE INDIVIDUAL ERNEST A. HAYGOOD, 1st Lt, USAF		22b. TELEPHONE (Include Area Code) (513) 255-2259	22c. OFFICE SYMBOL AFIT/CI

To my father

**INTERACTION OF ELECTROMAGNETIC
SIGNALS WITH PARTICULATE
CLOUDS**

by

JOSE MARIO PAUDA, B.S.

THESIS

Presented to the Faculty of the Graduate School of

The University of Texas at Austin

in Partial Fulfillment

of the Requirements

for the Degree of

MASTER OF ARTS

THE UNIVERSITY OF TEXAS AT AUSTIN

May, 1990

Accession For	
NTIS CRA&I	<input checked="" type="checkbox"/>
DTIC TAB	<input type="checkbox"/>
Unannounced	<input type="checkbox"/>
Justification	
By _____	
Distribution/	
Availability Codes	
Dist	Avail and/or Special
A-1	

Acknowledgments

It has been a pleasure to work with my supervisors, Dr Tom Griffy and Dr Dennis Wilson, both of whom have been extremely patient with me and very generous with their advice. Special thanks must go to Mr. Randy Roberts, a graduate student himself, who, despite his demanding course and research schedule, always took the time to answer my questions regarding the intricacies of the FORTRAN computer language and the details of the L^AT_EX document preparation system. Finally, my wife Blanca and son Francisco have my heartfelt thanks for enduring two years of graduate school.

JOSE MARIO PAUDA

The University of Texas at Austin

May, 1990

ABSTRACT

INTERACTION OF ELECTROMAGNETIC SIGNALS WITH PARTICULATE CLOUDS

by

JOSE MARIO PAUDA, B.S.

SUPERVISING PROFESSOR: THOMAS A. GRIFFY

A particulate cloud affects the ability of an electronic detector to receive an electromagnetic signal in two ways: by scattering light from the sun into the detector, thereby masking the signal, and by attenuating the signal itself. These effects are well studied in the Mie theory, which is summarized. The effect of the particle distribution in the cloud and the shape of the cloud on the scattering and absorption problems is then analyzed. The results of this analysis and of the Mie theory are incorporated into a computer program which is included in the appendix. The graphs generated with the program can be used (in conjunction with information about the sunlight intensity and the

detector's discriminating ability) to determine the effect of scattered light on the detection of the signal. We conclude that attenuation of the signal plays a relatively minor role in the ability of a detector to receive a signal affected by a cloud of particles.

Table of Contents

Acknowledgments	iv
ABSTRACT	v
Table of Contents	vii
List of Figures	ix
1. Introduction	1
1.1 Scattering: A New Computer Model for an Old Problem	1
1.2 Exact Solution to the Problem: The Mie Theory	2
1.2.1 Maxwell's Equations in the Scattering Medium	5
1.2.2 Solution of the Wave Equation in Spherical Coordinates	8
1.2.3 Boundary Conditions Between Different Media	11
1.2.4 The Mie Coefficients: Parameters in terms of Known Quantities	14
2. Particle Distributions and Cloud Shapes	17
2.1 Scattered and Absorbed Signals in Clouds with Nonuniform Particle Distributions	17
2.2 Determination of Particle Population	20
2.3 Effect of the Cloud Shape	23

3. Data Used, Results and Calculations	28
3.1 Data and Method of Calculation	28
3.2 Results of the Models	32
3.3 Conclusions	34
3.4 Recommendations for Further Work	34
A. The Computer Program	40
BIBLIOGRAPHY	66
Vita	

List of Figures

1.1	Relation between the incoming wave and the scattering angle . . .	3
1.2	A spherical coordinate system	9
1.3	Infinitesimal Gaussian pillbox	12
1.4	Infinitesimal Stokesian loop	13
2.1	Particle distribution for a Titan-IIIC rocket motor	22
2.2	A detector in a spherical cloud	24
2.3	The cloud as a cone	26
2.4	The detector's view axis off the y-z plane.	27
3.1	The imaginary part of the index of refraction for aluminum oxide at 2950 K	30
3.2	The real part of the index of refraction for aluminum oxide at 2950 K	31
3.3	$\frac{I}{I_0}$ for the aluminum oxide particle distribution of a Titan-IIIC rocket at $\lambda = 4.04 \mu\text{m}$	35
3.4	$\frac{I}{I_0}$ for the aluminum oxide particle distribution of a Titan-IIIC rocket at $\lambda = 6.25 \mu\text{m}$	36
3.5	$\frac{I}{I_0}$ for the aluminum oxide particle distribution of a Titan-IIIC rocket at $\lambda = 8.0 \mu\text{m}$	37

3.6 $\frac{I}{I_0}$ for the smoke particle distribution of a Titan-III C rocket at
 $\lambda = 10.0 \mu\text{m}$ 38

3.7 The attenuation for the aluminum oxide and smoke particle dis-
tribution of a Titan-III C rocket at $\lambda = 8.0 \mu\text{m}$ and $\lambda = 10.0 \mu\text{m}$,
respectively. 39

Chapter 1

Introduction

1.1 Scattering: A New Computer Model for an Old Problem

Most of the information we receive from a variety of sources is in the form of electromagnetic signals. These electromagnetic signals interact with the particles suspended in the medium through which they travel. Examples include the absorption of sunlight by dust particles suspended in the atmosphere, the absorption of radar signals by water droplets, and the absorption of infrared signals by particles produced by rocket motors. If we assume that an electronic detector is to receive and process a signal that has to interact with a cloud, be it a radar return passing through a rain cloud or an infrared signature of a "hot" object passing through a smoke cloud, we must investigate the effect of the particulate cloud on the signal itself. This effect is two-fold: the signal may be partially absorbed by the particles to a point below the threshold of the detector, or the signal may be masked by the light from a brighter source scattered by the particles into the detector. This is the major aim of this project: to create a computer model to investigate the absorption (also called the extinction) of the signal as it travels through a cloud of particles and the masking of the signal by light scattered by a cloud of particles. Specifically, we consider the effect a conical cloud has on a detector at the vertex of the cloud. This investigation is by no means new. However, other authors have

limited their investigations to long wavelengths or to preselected absorption values. We have tried to fill this gap by providing a general computer code, with none of the limitations listed above. Thus, by implementing the code included in the appendix, the reader will be able to generate theoretical predictions for a wide range of particles, wavelengths and refraction coefficients. In the remainder of this chapter, a brief explanation of how these parameters affect the absorption and scattering of the signal is presented. In particular, the results of the Mie Theory are summarized and expressions for the electric and magnetic fields in terms of known parameters are presented. In chapter 2 the effect a nonconstant particle size distribution is investigated, as well as the effect of the shape of the cloud itself. In chapter 3 we apply the information from chapters 1 and 2 and present the graphs of the scattered light and absorbed signal. These graphs were obtained by plotting the points calculated by the computer program included in the appendix.

1.2 Exact Solution to the Problem: The Mie Theory

Any electromagnetic signal may be treated as a plane wave if the distance from the source to the observation point is much greater than the wavelength. More explicitly, if the observation point is at a distance d from the source and the signal has wavelength λ , then with $k = \frac{2\pi}{\lambda}$, the signal may be treated as a plane wave if

$$kd \gg 1. \tag{1.1}$$

In particular, consider a spherical particle in a vacuum at a distance d from the sun, such that equation 1.1 holds. Furthermore, assume that the particle is

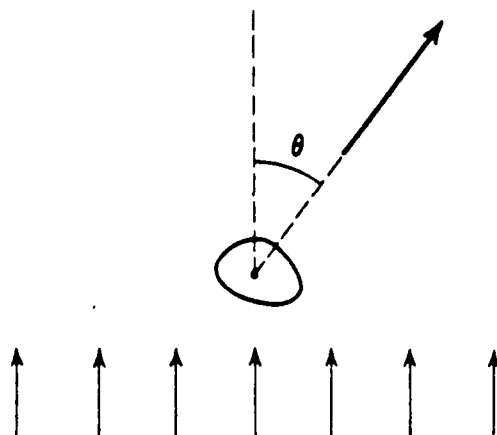


Figure 1.1: Relation of the incoming plane wave to the scattering angle θ [van de Hulst 81, page 12].

absorbing in the infrared region of the spectrum. Then the scattering problem is as depicted in figure 1.1: a train of plane waves comes in from “infinity” and interacts with the particle. Part of the signal is absorbed and part is scattered at an angle θ . If the radius of the particle is much smaller than the wavelength, $r \ll \lambda$, the problem reduces to the well-known Rayleigh scattering, treated in many textbooks. Jackson, for instance, has several sections dedicated to this very problem [Jackson 75, sections 9.6 and 9.7]. However, to solve the scattering problem exactly, with no assumptions as to the ratio of the particle’s size to the wavelength of the signal, we must solve Maxwell’s equations subject to the appropriate boundary conditions. This problem was first solved by Mie in 1908 [Mie 08]. In his classic book van de Hulst covers the work of Mie thoroughly and concisely [van de Hulst 81, chapter 9]. Indeed, his treatment of the scattering of light is among the most lucid and complete. In this thesis, we do not recreate Mie’s original work, nor emulate van de Hulst’s. Instead, we simply summarize the process they used to arrive at the solution. Their result

is then used to write the computer program which can be used to calculate the effects of a cloud of particles on the signal.

Consider, then, a plane wave of random polarization, and a spherical particle with which the wave interacts, as in figure 1.1. Let the electric field be represented by \mathbf{E} and the magnetic field be represented by \mathbf{B} . Furthermore, let the wave have wavelength λ and circular frequency $\omega = ck$. Then, in any medium, this wave is represented by Maxwell's equations as¹

$$\nabla \cdot \mathbf{E} = 0 \quad \nabla \times \mathbf{E} + \frac{1}{c} \frac{\partial \mathbf{B}}{\partial t} = 0$$

$$\nabla \cdot \mathbf{B} = 0 \quad \nabla \times \mathbf{B} - \frac{\mu\epsilon}{c} \frac{\partial \mathbf{E}}{\partial t} = 0$$

where c is the speed of light in vacuum, μ is the magnetic permeability and ϵ is the electric permittivity of the medium (in vacuum, these parameters are unity). By combining the two curl equations, we can show that each cartesian component of \mathbf{E} and \mathbf{B} satisfies the wave equation

$$\nabla^2 u - \frac{1}{v^2} \frac{\partial^2 u}{\partial t^2} = 0 \tag{1.2}$$

where

$$v = \frac{c}{\sqrt{\mu\epsilon}} \tag{1.3}$$

is the velocity of the wave in the medium. For a wave traveling in the z direction, the wave equation 1.2 has the solution

$$u(z, t) = e^{-ikz+i\omega t}. \tag{1.4}$$

¹In this introductory chapter, we follow the approach of van de Hulst, chapter 9. In particular, we use his notation for a plane wave traveling in the z direction as shown in equation 1.4. Most modern references assign a negative sign to the time component of the wave and a positive sign to the spacial component, which is opposite to the convention adopted here. In addition, we have used the cgs unit system.

This solution may be generalized to include the vector quality of the \mathbf{E} and \mathbf{B} fields. Following the convention that the physical electric and magnetic fields are obtained by taking the real parts of complex quantities, the plane wave fields may be written in the form

$$\mathbf{E}(z, t) = \mathbf{e}_1 E e^{-ikz + i\omega t} \quad (1.5)$$

$$\mathbf{B}(z, t) = \mathbf{e}_2 B e^{-ikz + i\omega t} \quad (1.6)$$

Equations 1.5 and 1.6 describe a plane, transverse wave in vacuum, with the electric field, of magnitude E , polarized in the \mathbf{e}_1 direction and the magnetic field, of magnitude B , pointing in the \mathbf{e}_2 direction. The waves then interact with the particle, resulting in an outgoing-scattered wave as shown in figure 1.1. The rigorous solution of the problem requires the matching of boundary conditions at the surface of the particle between the outside-incident wave and the inside wave, and the inside wave and the outside-scattered wave. Therefore, we must investigate the nature of the waves in the medium as well as the nature of the boundary conditions. We do this in the next three subsections.

1.2.1 Maxwell's Equations in the Scattering Medium

To find the nature of the electromagnetic waves in the medium, we must solve Maxwell's equations as they are expressed in the medium itself. Consider, then, a plane wave of random polarization, and a spherical particle with which the wave interacts, as in figure 1.1. In the scatterer itself, or put differently, in a macroscopic medium with surface charge density ρ and current \mathbf{J} , Maxwell's equations are

$$\nabla \cdot \mathbf{D} = 4\pi\rho \quad (1.7)$$

$$\nabla \times \mathbf{E} = -\frac{1}{c} \frac{\partial \mathbf{B}}{\partial t} \quad (1.8)$$

$$\nabla \cdot \mathbf{B} = 0 \quad (1.9)$$

$$\nabla \times \mathbf{H} = \frac{1}{c} \frac{\partial \mathbf{D}}{\partial t} + \frac{4\pi}{c} \mathbf{J} \quad (1.10)$$

where \mathbf{H} is the magnetic field, \mathbf{B} is the magnetic induction, \mathbf{E} is the electric field, and \mathbf{D} is the electric displacement. The electric displacement and electric field are related by

$$\mathbf{D} = \epsilon \mathbf{E}, \quad (1.11)$$

while the magnetic field and magnetic induction are given by

$$\mathbf{H} = \frac{1}{\mu} \mathbf{B}. \quad (1.12)$$

Finally, the current \mathbf{J} and the electric field \mathbf{E} are related by Ohm's Law:

$$\mathbf{J} = \sigma \mathbf{E}, \quad (1.13)$$

where σ is the conductivity of the medium. In section 1.2 we assumed that, before interaction with the scatterer, the magnetic and electric fields form a plane wave. We also found that they are periodic in nature, given by equations 1.5 and 1.6. When they interact with the scatterer, the expression for the \mathbf{E} and \mathbf{H} fields changes (as we shall see). Nonetheless, they maintain their periodic nature. Thus, in the scatterer, the magnetic and electric fields are of the form

$$\mathbf{E} = \mathbf{E}_o(x) \exp^{i\omega t} \quad (1.14)$$

$$\mathbf{H} = \mathbf{H}_o(x) \exp^{i\omega t}, \quad (1.15)$$

where $\mathbf{E}_o(x)$ and $\mathbf{H}_o(x)$ are the complex amplitudes. By taking the time derivatives of equation 1.14 and equation 1.15 above, plugging into the two

curl equations (equations 1.8 and 1.10) and simplifying, we obtain

$$\nabla \times \mathbf{E} = -ik\mathbf{H} \quad (1.16)$$

and

$$\nabla \times \mathbf{H} = ikm^2\mathbf{E}, \quad (1.17)$$

where $\mathbf{J} = \sigma\mathbf{E}$ and $\mathbf{D} = \epsilon\mathbf{E}$ have been used. The new term m in equation 1.17 is called the *complex index of refraction*, given by²

$$m^2 = \epsilon - \frac{4\pi i\sigma}{\omega}, \quad (1.18)$$

while $k = \frac{2\pi}{\lambda}$. From equation 1.18 it is apparent that the complex index of refraction is a function of frequency. However, in practical applications, " m cannot generally be determined from the static values of ϵ and σ but should be determined by measurements at the circular frequency ω " [van de Hulst 81, page 116].

The curl equations remain coupled. However, by applying the divergence equations, we can decouple them as follows. From equation 1.17 we get

$$\mathbf{E} = \frac{-i}{km^2} \nabla \times \mathbf{H}.$$

Taking the curl,

$$\nabla \times \mathbf{E} = \frac{-i}{km^2} \nabla \times (\nabla \times \mathbf{H}),$$

²In so defining m , we have separated the complex part of the problem from the wave number k . Other authors, Jackson in particular, prefer to include the complex factor in the k itself [Jackson 75, page 286]. Thus, what we denote as mk is equivalent to Jackson's k . Furthermore, our expression for m will not involve the parameter μ , since we shall restrict our analysis to substances for which $\mu = 1$.

or, using $\nabla \cdot \mathbf{H} = \frac{1}{\mu} \nabla \cdot \mathbf{B} = 0$,

$$\nabla \times \mathbf{E} = \frac{i}{km^2} \nabla^2 \mathbf{H}. \quad (1.19)$$

Equating equation 1.16 to equation 1.19 and rearranging terms, we get an expression involving only the magnetic field \mathbf{H} :

$$\nabla^2 \mathbf{H} + k^2 m^2 \mathbf{H} = 0. \quad (1.20)$$

A similar (decoupled) equation can be obtained for the electric field, \mathbf{E} . Thus, each of the cartesian coordinates of \mathbf{E} and \mathbf{H} satisfy the *scalar* wave equation

$$\nabla^2 u + k^2 m^2 u = 0. \quad (1.21)$$

The simplest solution to the scalar wave equation is very enlightening. This simple solution is

$$u(z, t) = e^{-ikmz + i\omega t}.$$

Notice that, if m has an imaginary component, then the wave in the medium of propagation is damped. On the other hand, if m is strictly real, the wave suffers no attenuation, although it does undergo a phase shift. As enlightening as this form of the solution might be, however, it does not represent the solution of the wave in a spherical particle, nor the solution of the wave scattered by a small sphere. The actual solution involves spherical waves, which is the topic of the next section.

1.2.2 Solution of the Wave Equation in Spherical Coordinates

Consider the spherical coordinates shown in figure 1.2. Assuming that

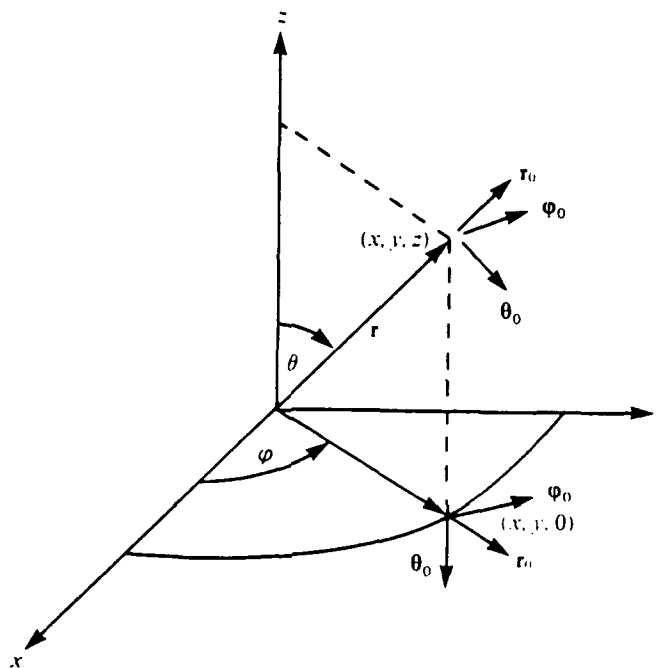


Figure 1.2: A spherical coordinate system. The origin of the system is located at the center of the scattering sphere [Arfken 85, page 104].

the scalar wave equation is separable in r , θ and ϕ , its solution may be written as

$$u(r, \theta, \phi) = R(r)\Theta(\theta)\Phi(\phi).$$

Using the laplacian for spherical coordinates, separating the radial equation from the angular dependence, and solving the resulting three equations, we obtain³

$$u(r, \theta, \phi) = (A \cos(l\phi) + B \sin(l\phi))P_n^l(\cos \theta)z_n(mkr),$$

where A and B are constants, l and n are integers such that

$$n \geq l \geq 0,$$

$P_n^l(\cos \theta)$ is the associated Legendre polynomial, and $z_n(mkr)$ is the spherical Bessel function.

Since the scalar vector function represents any one of the components of the vector wave function, it follows that the solution of the scalar function *must* be related to the solution of the vector wave function. Mie shows that, if u is a solution of the scalar wave function, then the vectors M_u and N_u , defined by

$$M_u = \nabla \times (ru) \tag{1.22}$$

and

$$mkN_u = \nabla \times M_u, \tag{1.23}$$

satisfy the *vector* wave equation. Furthermore, M_u and N_u are related by

$$mkM_u = \nabla \times N_u \tag{1.24}$$

³The separation of variables in spherical coordinates is treated in many textbooks. See, for instance, [Slater 47, pages 148 to 151] and [Arfken 85, page 105 and pages 448 to 450].

Finally, if u and v are two independent solutions to the scalar wave function, then the electric and magnetic fields are given by

$$\mathbf{E} = M_v + iN_u \quad (1.25)$$

and

$$\mathbf{H} = m(-M_u + iN_v), \quad (1.26)$$

respectively [Mie 08, page 120]. Thus, given two independent solutions to the scalar wave equation of a wave in an absorbing medium, we can find the electric and magnetic fields which satisfy the vector wave equation. However, the wave equation need not be limited to a dissipative medium. Equations 1.22 through 1.26 apply equally well to an incoming (*incoming* from the point of view of a scatterer) plane wave in vacuum, as well as to an outgoing, scattered, spherical wave, provided m is appropriately expressed. The exact relationship between these waves is given by matching the appropriate boundary conditions at the skin of the scatterer. The nature of these boundary conditions is the subject of the next section.

1.2.3 Boundary Conditions Between Different Media

Equations 1.7 through 1.10 are the differential form of Maxwell's equations for waves in a macroscopic medium. By applying the divergence and Stoke's theorem, Maxwell's equations can be written in their integral form:

$$\oint_S \mathbf{D} \cdot \mathbf{n} da = 4\pi \int_V \rho d^3x \quad (1.27)$$

$$\oint_S \mathbf{B} \cdot \mathbf{n} da = 0 \quad (1.28)$$

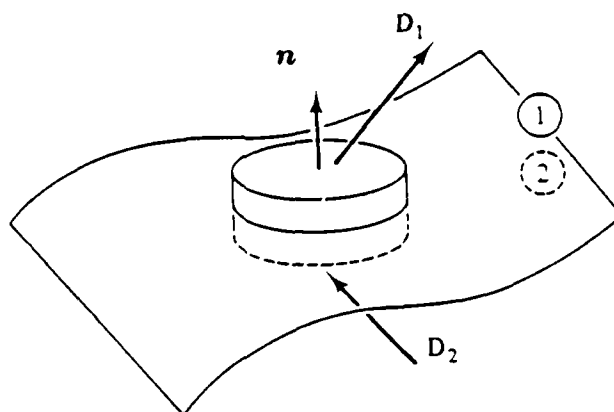


Figure 1.3: Infinitesimal Gaussian pillbox used to determine boundary conditions [Griffiths 81, page 280].

$$\oint_C \mathbf{H} \cdot d\mathbf{l} = \int_S \left[\frac{4\pi}{c} \mathbf{J} + \frac{1}{c} \frac{\partial \mathbf{D}}{\partial t} \right] \cdot \mathbf{n} da \quad (1.29)$$

$$\oint_C \mathbf{E} \cdot d\mathbf{l} = -\frac{1}{c} \int_S \frac{\partial \mathbf{B}}{\partial t} \cdot \mathbf{n} da, \quad (1.30)$$

where equations 1.27 and 1.28 are defined over any closed surface S with volume V , and equations 1.29 and 1.30 are over any surface S bounded by the closed loop C . In this form, Maxwell's equations are particularly useful in determining the boundary conditions.⁴ Consider a very thin Gaussian pillbox as in figure 1.3. As the thickness of the pillbox goes to zero, equation 1.27 leads to

$$(\mathbf{D}_2 - \mathbf{D}_1) \cdot \mathbf{n} = 4\pi \Sigma, \quad (1.31)$$

⁴Griffiths gives a particularly good presentation of the limiting process used to arrive at the boundary conditions [Griffiths 81, pages 280 and 281, and, on a different context, pages 78 and 79].

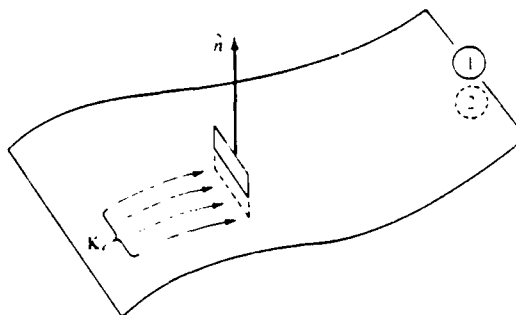


Figure 1.4: Infinitesimal Stokesian loop used to determine boundary conditions [Griffiths 81, page 281].

where Σ is the surface charge density. Meanwhile, equation 1.28 leads to

$$(\mathbf{B}_2 - \mathbf{B}_1) \cdot \mathbf{n} = 0. \quad (1.32)$$

Similarly, consider the Stokesian loop in figure 1.4. As the height goes to zero, equation 1.30 leads to

$$\mathbf{n} \times (\mathbf{E}_2 - \mathbf{E}_1) = 0, \quad (1.33)$$

while equation 1.29 leads to

$$\mathbf{n} \times (\mathbf{H}_2 - \mathbf{H}_1) = \frac{4\pi}{c} \mathbf{K}_f, \quad (1.34)$$

where \mathbf{K}_f is the idealized surface current. If medium 1 has an index of refraction m_1 and medium 2 has an index of refraction m_2 , both finite, then the surface current \mathbf{K}_f vanishes [van de Hulst 81, page 117]. Then, equation 1.34 may be written as

$$\mathbf{n} \times (\mathbf{H}_2 - \mathbf{H}_1) = 0 \quad (1.35)$$

Equations 1.31, 1.32, 1.33 and 1.35 are the boundary equations to which the incoming, inside and outgoing wave are subject. To find the scattered electric and magnetic fields at any point in space, all that remains to be done is to find the waves in terms of known quantities and apply the boundary conditions. We do this in the next section.

1.2.4 The Mie Coefficients: Parameters in terms of Known Quantities

A review of the progress achieved seems appropriate at this point⁵. So far, we have found an expression for the plane waves in vacuum (equations 1.5 and 1.6) which then interact with the spherical scatterer. We have found (equations 1.25 and 1.26) the expression for the electric and magnetic fields inside and outside the scatterer in terms of two linearly independent scalar functions u and v (these scalar functions are to be determined). We have also discussed the boundary conditions which the incoming wave, the inside and the scattered wave must satisfy (equations 1.31, 1.32, 1.33 and 1.35). In this last section of this introductory chapter, we apply the boundary conditions to obtain the solution to the scattering problem in terms of known quantities. First, however, we must find the expression for the scalar functions u and v . As explained in [van de Hulst 81, pages 121 through 123] the electric and magnetic fields may be expressed in terms of the scalar functions u and v as follows.

⁵The credit goes to Mie, of course. In this section we continue to summarize his theory, as presented by van de Hulst.

The outside, incident wave:

$$u = e^{i\omega t} \cos(\phi) \sum_{n=1}^{\infty} (-i)^n \frac{2n+1}{n(n+1)} P_n^1(\cos\theta) j_n(kr), \quad (1.36)$$

$$v = e^{i\omega t} \sin(\phi) \sum_{n=1}^{\infty} (-i)^n \frac{2n+1}{n(n+1)} P_n^1(\cos\theta) j_n(kr). \quad (1.37)$$

The angles ϕ and θ are as defined in figure 1.2, n is an integer from 0 to ∞ , j_n is the spherical Bessel function of the first kind and $P_n^1(\cos\theta)$ is the associated Legendre polynomial.

The inside wave:

$$u = e^{i\omega t} \cos(\phi) \sum_{n=1}^{\infty} m c_n (-i)^n \frac{2n+1}{n(n+1)} P_n^1(\cos\theta) j_n(mkr), \quad (1.38)$$

$$v = e^{i\omega t} \sin(\phi) \sum_{n=1}^{\infty} m d_n (-i)^n \frac{2n+1}{n(n+1)} P_n^1(\cos\theta) j_n(mkr), \quad (1.39)$$

and the outside, scattered wave

$$u = e^{i\omega t} \cos(\phi) \sum_{n=1}^{\infty} -a_n (-i)^n \frac{2n+1}{n(n+1)} P_n^1(\cos\theta) h_n^{(2)}(kr), \quad (1.40)$$

$$v = e^{i\omega t} \sin(\phi) \sum_{n=1}^{\infty} -b_n (-i)^n \frac{2n+1}{n(n+1)} P_n^1(\cos\theta) h_n^{(2)}(kr), \quad (1.41)$$

where $h_n^{(2)}(kr)$ is the spherical Hankel function of the second kind. In the equations for the inside and the scattered waves, (equations 1.38 through 1.41) a_n , b_n , c_n and d_n are called the Mie coefficients. These coefficients are the sought-after parameters which are expressed in terms of known (or functions of known) quantities. By matching the appropriate boundary conditions at the

skin of the particle (see section 1.2.3), we obtain for the Mie coefficients

$$a_n = \frac{S'_n(y)S_n(x) - mS_n(y)S'_n(x)}{S'_n(y)\zeta_n(x) - mS_n(y)\zeta'_n(x)}, \quad (1.42)$$

$$b_n = \frac{mS'_n(y)S_n(x) - S_n(y)S'_n(x)}{mS'_n(y)\zeta_n(x) - S_n(y)\zeta'_n(x)}. \quad (1.43)$$

where $x = ka = \frac{2\pi a}{\lambda}$, $y = mka$, and m is the complex index of refraction of the medium. S_n and C_n are the Riccati-Bessel functions defined by

$$S_n(z) = zj_n(z), \quad (1.44)$$

and

$$C_n(z) = -zn_n(z). \quad (1.45)$$

where $j_n(z)$ and $n_n(z)$ are the spherical Bessel functions of the first and second kind, respectively⁶. The function $\zeta(n)$ is defined in terms of S_n and C_n :

$$\zeta(z) = S_n(z) + iC_n(z).$$

Thus, for a given radius r , a wavelength λ , and a complex index of refraction m , we can find the corresponding Mie coefficients. Having found the Mie coefficients, we can then find the fields at any point. However, the distribution of the size of the particles in the cloud, the shape of the cloud and, most importantly, the direction in which the detector is "looking," make the problem nontrivial. In the next chapter we investigate these factors.

⁶See section 3.1 for the generating function used for the Riccati-Bessel functions.

Chapter 2

Particle Distributions and Cloud Shapes

2.1 Scattered and Absorbed Signals in Clouds with Nonuniform Particle Distributions

In problems of practical importance, the signal is affected by a *cloud* of particles, as opposed to just one particle. Recall the problem at hand: a signal may be masked by the light from a strong source scattered into the detector, or the signal itself may be attenuated by the cloud. Although the cloud may have any geometrical shape, the particles tend to be spherical.¹ If we further assume, for now, that all particles in the cloud have radius a and that the number of particles per unit volume is N , then the light intensity scattered per unit volume in the direction θ , is

$$I_{total}(\theta, a) = NI(\theta, a) \quad (2.1)$$

where $I(\theta, a)$ is the intensity of light scattered by one particle. In terms of the Mie coefficients, the intensity is given by²

$$I(\theta, a) = I_0 \frac{i_1(\theta) + i_2(\theta)}{2k^2 r^2}, \quad (2.2)$$

¹This certainly seems true of particles produced by rocket motors. See, for instance, [Dawbarn 80].

²On first inspection, it seems as though the intensity $I(\theta, a)$ is *not* a function of the radius a of the particle. However, we must keep in mind that the Mie coefficients, which are a part of i_1 and i_2 by equations 2.2 through 2.6, are radius-dependent.

where r is the distance from the detector to the scatterer, I_0 is the intensity of the incident wave, and $i_1(\theta)$ and $i_2(\theta)$ are the scattering functions for the perpendicular and plane polarized scattered waves, respectively. They are given by

$$i_1(\theta) = |\mathcal{S}_1(\theta)|^2, \quad (2.3)$$

and

$$i_2(\theta) = |\mathcal{S}_2(\theta)|^2. \quad (2.4)$$

In turn, $\mathcal{S}_1(\theta)$ and $\mathcal{S}_2(\theta)$ are given by³

$$\mathcal{S}_1(\theta) = \sum_{n=1}^{\infty} \frac{2n+1}{n(n+1)} \{a_n \pi_n(\cos \theta) + b_n \tau_n(\cos \theta)\}, \quad (2.5)$$

and

$$\mathcal{S}_2(\theta) = \sum_{n=1}^{\infty} \frac{2n+1}{n(n+1)} \{b_n \pi_n(\cos \theta) + a_n \tau_n(\cos \theta)\}. \quad (2.6)$$

Finally, $\pi_n(\cos \theta)$ and $\tau_n(\cos \theta)$ are given by

$$\pi_n(\cos \theta) = \frac{dP_n(\cos \theta)}{d \cos \theta}, \quad (2.7)$$

and

$$\tau_n(\cos \theta) = \cos(\theta) \pi_n(\cos \theta) - \sin^2 \theta \frac{d\pi_n(\cos \theta)}{d \cos \theta}, \quad (2.8)$$

where $P_n(\cos \theta)$ is the Legendre polynomial of order n . The second part of the problem involves the attenuation of the signal itself. This attenuation is given by

$$I = I_0 e^{-\gamma R}, \quad (2.9)$$

³The functions \mathcal{S}_1 and \mathcal{S}_2 are not to be confused with the Riccati-Bessel functions S_n defined by equation 1.44.

where R is the distance the signal has traveled in the absorbing cloud, and γ is the *extinction coefficient*, which is a function of the size of the particles, a , the number of particles per unit volume, N , and the *extinction efficiency factor*, Q_{ext} :

$$\gamma = N\pi a^2 Q_{ext}. \quad (2.10)$$

In terms of the Mie coefficients, the extinction efficiency factor is given by

$$Q_{ext} = \frac{2}{x^2} \sum_{n=1}^{\infty} (2n+1) \operatorname{Re}(a_n + b_n) \quad (2.11)$$

Finally, in the above equation, x is the ratio of the particle's circumference to the wavelength of the light:

$$x = \frac{2\pi a}{\lambda} \quad (2.12)$$

Realistically, however, the particles in the cloud will be of different sizes. The number of particles per unit volume of a given radius is determined by a distribution function. The number density of particles with radii between a and $a + da$ (as given by the distribution) replaces N in formulas 2.1 and 2.10. The effect of the whole cloud is obtained by adding the contributions of all the individual parts. For instance, for the total intensity of the light scattered in the direction θ , the expression is

$$I_{total}(\theta) = \sum_i I_i(\theta, a_i) \quad (2.13)$$

where $I_i(\theta, a_i)$ is the intensity of light scattered at an angle θ by particles of radius a_i . Similarly, the total attenuation coefficient γ becomes

$$\gamma = \int_0^{\infty} Q_{ext}(a) \frac{\Delta N}{\Delta a}(a) \pi a^2 da, \quad (2.14)$$

where $\frac{\Delta N}{\Delta a}(a)$ represents the normalized particle size distribution:

$$\int_0^{\infty} \frac{\Delta N}{\Delta a}(a) da = 1.$$

$\frac{\Delta N}{\Delta a}(a)da$, then, represents the number of particles with radii between a and $a + da$ per unit volume. In the next section we will find the actual particle population for a given distribution.

2.2 Determination of Particle Population

Throughout this paper, we have summarized the results of the Mie theory and treated the scattering of an electromagnetic signal in very general terms. We will now specialize the discussion to the cloud of aluminum oxide particles found in the exhaust of rockets. The aluminum oxide is produced as a byproduct of aluminized solid fuel used to propel the rockets. As the fuel burns, the aluminum particles in the propellant vaporize and react with oxygen to form molten aluminum oxide [Mularz 72]. This example is of current interest, for it applies, among other problems, to the recovery of satellites by the Space Shuttle. One of the missions of the Shuttle is to recover satellites before they fall back to the Earth. If the satellite has not been visually detected (or cannot be visually detected due to distance, operational constraints, etc.), then it must be detected by the infrared signature the satellite possesses. If the Shuttle is firing its rockets to maneuver, then the signal may have to pass through the cone-shaped cloud of the Shuttle's exhaust. The size of the particles in the cloud will not be of one, and only one, radius. They will, instead, be distributed throughout a wide range of values. However, to illustrate the method used to obtain the solution for a non-constant distribution, we first look at the simplest

of distributions: a constant distribution. Assuming there are \mathcal{N} particles of density ρ and constant radius a , the total mass M of the particles is⁴

$$M = \mathcal{N} \frac{4}{3} \pi a^3 \rho.$$

Solving for \mathcal{N} , the total number of particles,

$$\mathcal{N} = \frac{M}{\frac{4}{3} \pi a^3 \rho}.$$

This result is most useful if expressed as a particle density:

$$N = \frac{M}{\frac{4}{3} \pi a^3 \rho} \frac{1}{Volume_{cloud}},$$

where N represents the number of particles per unit volume and $Volume_{cloud}$ depends on the shape of the cloud.

For a non-constant distribution, we must take a weighted average. Consider, for example, the following distribution, which is the distribution of particles produced by the Titan-IIIC rocket exhaust⁵:

$$\frac{\Delta \mathcal{N}}{\Delta a}(a) = 0.012(2a)^2 \exp[-1.89 \times 10^{-2}(2a)^2], \quad (2.15)$$

which is shown in figure 2.1. By definition of a distribution, $\Delta \mathcal{N}(a_i)$ is the number of particles with radii between a_i and $a_i + \Delta a$. Let $vol(a_i)$ be the

⁴Notice that the actual *number* of particles is denoted by \mathcal{N} , while the number *density* is denoted by N .

⁵It may seem as though we are using one system (the Titan-IIIC rocket) to talk about another system (the Space Shuttle). However, the reader must bear in mind that the Shuttle was introduced only as an example. Certainly, there must be other examples to which this analysis applies. Furthermore, the distribution of the Shuttle's exhaust must resemble, at least in shape, the distribution presented in figure 2.1

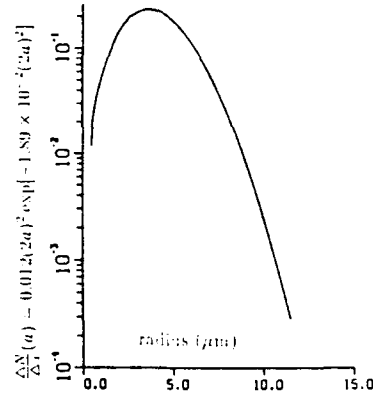


Figure 2.1: Particle distribution for a Titan-IIIC rocket motor [Dawbarn 80, page 126].

volume of the particles with radii between a_i and $a_i + \Delta a$. Then the mass of all the particles present is

$$M = \sum_i vol(a_i) \rho \Delta \mathcal{N}(a_i)$$

$$M = \rho \sum_i vol(a_i) \Delta \mathcal{N}(a_i).$$

Solving for $\Delta \mathcal{N}(a_i)$, we get

$$\Delta \mathcal{N}(a_i) = \frac{M}{\rho \sum_i vol(a_i)}. \quad (2.16)$$

We have assumed, for simplicity, that all the burned mass turns to smoke particles or other absorbing particles. This is usually not the case. Instead, only a fraction f of the amount burned turns into particles. Thus equation 2.16, expressed as a number density, becomes

$$\Delta N(a_i) = \frac{fM}{\rho \sum_i vol(a_i) Volume_{cloud}}, \quad (2.17)$$

where $\Delta N(a_i)$ is the number of particles per unit volume with radii between a_i and $a_i + \Delta a$. To encode the above ideas into a computer program, we need

to write a program to solve the scattering/absorption problem for a "constant" distribution. We then take care of the changing nature of the distribution by incrementing the radius a small amount, and solving that "constant" distribution problem. However, the amount of light (scattered or absorbed) reaching the detector depends not only on the distribution of particles in the cloud, but also on the shape of the cloud itself. We investigate the effect of the cloud on the signal in the next section.

2.3 Effect of the Cloud Shape

We now turn to the question of the effect the shape of the cloud has on the scattering and absorption of light. Again, we start with a very simple model: a detector at the center of a spherical cloud composed of constant size particles. Figure 2.2 shows the arrangement. In this case there is perfect symmetry. The intensity of the scattered light reaching the detector is the intensity of the light in the solid angle subtended by the cone:

$$I = 2\pi \int_0^{R_c} r^2 dr \int_{\theta_1}^{\theta_2} \sin \theta d\theta \frac{i(\theta)}{r^2}. \quad (2.18)$$

Substituting equation 2.2 for the intensity $i(\theta)$ in equation 2.18, we can express the ratio of the scattered intensity to the original intensity as

$$\frac{I}{I_0} = \frac{N\pi R_c}{k^2} \int_{\theta_1}^{\theta_2} \sin(\theta)(i_1(\theta') + i_2(\theta'))d\theta, \quad (2.19)$$

where θ is the angle the detector makes with the z axis, θ' is the scattering angle, $\theta' = \pi - \theta$, and $\Delta\theta = \theta_2 - \theta_1$ is the resolution angle of the detector (see figure 2.2). Recall that $i_1(\theta)$ and $i_2(\theta)$ are functions of the Mie coefficients (see equations 2.3 through 2.6). Thus, *all the parameters in equation 2.19 are*

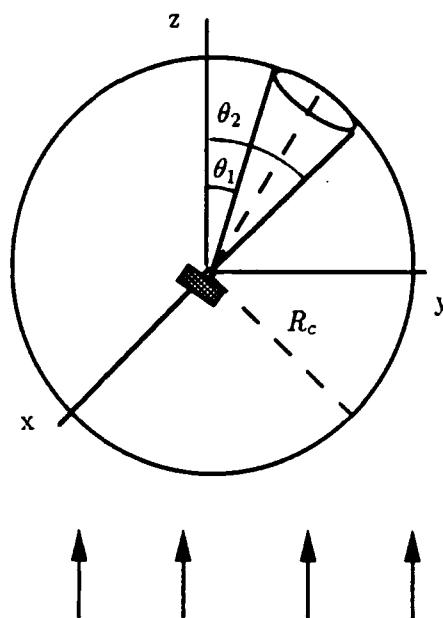


Figure 2.2: A detector in a spherical cloud. The intensity reaching the detector is the intensity of light in the solid angle subtended by the detector's field of view.

known. Consequently, for a given size particle, we now have an expression for the scattered intensity (the absorption of the signal remains as given by equations 2.9 through 2.12). For a distribution of particles with n different sizes, we simply repeat the process n times, each time with the appropriate particle radius.

For a cone-shaped cloud, the problem is, in many respects, similar to the problem of the spherical cloud—and uniquely different in others. For instance, if the solid angle subtended by the detector's view angle is completely contained within the conical cloud, then the problem is identical to the spherical-cloud problem—with the provision that the particle density will be higher for the cone cloud because of its smaller volume for compatible dimensions (see figure 2.3). However, if the detector is “looking” off the axis of the cloud, as in figure 2.4, then the problem loses all resemblance to the spherical cloud problem and becomes much more complicated. Specifically, the intensity of the scattered light will depend on the following factors:

1. The relative sizes of the solid angle of the detector's field of view and the conical cloud.
2. The angle the axis of the cloud makes with the sun's rays (the z axis).
3. The viewing angle of the detector with respect to the axis of the cloud. This angle does not have to be in the same plane as the sun's rays and the axis of the cloud.

We treat the case in which conditions 1 and 2 above apply, with the detector's view axis on the z - y plane, as in figure 2.3. A detector view width of two

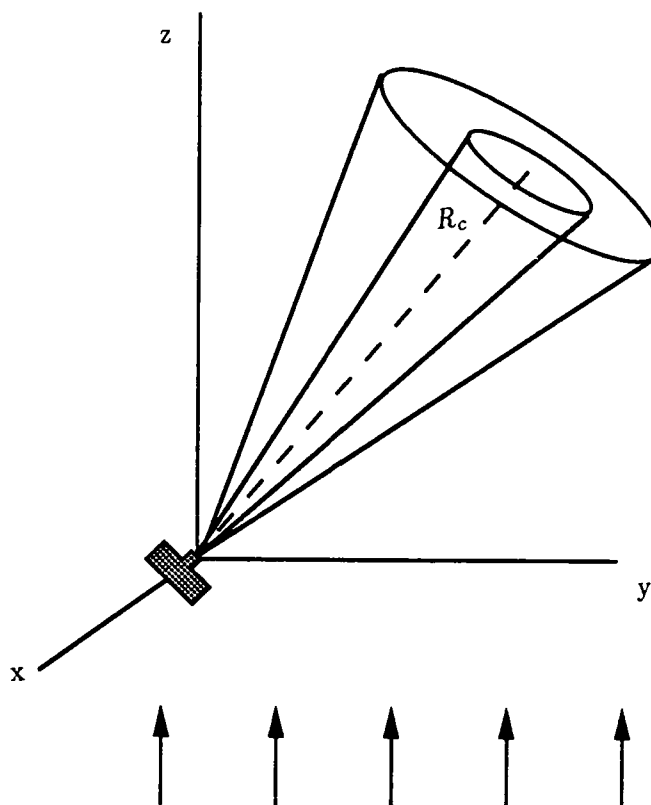


Figure 2.3: The cloud as a cone. The angle subtended by the detector is smaller than the angle subtended by the cloud

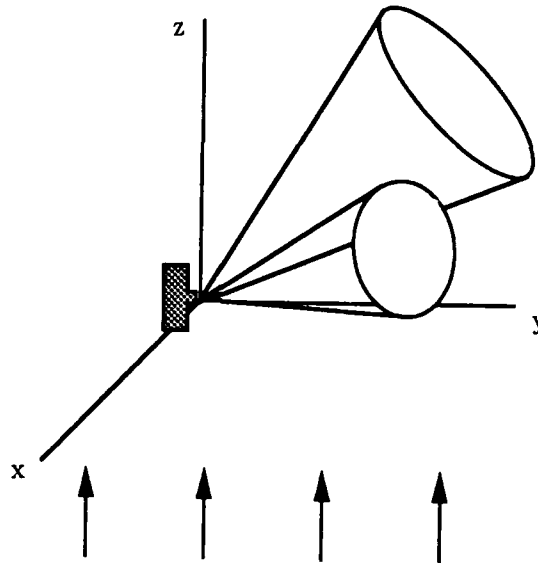


Figure 2.4: The detector's view axis off the y-z plane.

degrees is used, while the ratio of the length of the cone cloud to the radius of the base is set as 10 to 1, giving a cloud angle of 11 degrees. Thus, the detector's view angle is contained within the cloud.

Chapter 3

Data Used, Results and Calculations

3.1 Data and Method of Calculation

The computer program can be described as a series of iterations of the equations in chapters 1 and 2. Specifically, it divides the distribution function of the particles (smoke or aluminum oxide) into 50 equally spaced regions.¹ Thus, since it is assumed that the smallest radius in the distribution is zero and that the largest radius is 12 μm , the center of the i th division corresponds to a radius of $a_i = (i + \frac{1}{2})(0.24) \mu\text{m}$, or to a diameter of $D_i = (i + \frac{1}{2})(0.48) \mu\text{m}$. For each radius thus calculated, it finds the Mie coefficients using equations 1.42 and 1.43. The Riccati-Bessel functions used in equations 1.42 and 1.43 are generated using the following expressions, taken from [Gumprecht 51, pages xii and xiii]:

$$S_n(x) = \frac{2n-1}{x} S_{n-1}(x) - S_{n-2}(x), \quad (3.1)$$

and

$$C_n(x) = \frac{2n-1}{x} C_{n-1}(x) - C_{n-2}(x), \quad (3.2)$$

given that the two initial functions are given by

$$S_0(x) = \sin(x), \quad S_1(x) = \frac{\sin(x)}{x} - \cos(x),$$

¹We found that 50 iterations give results accurate to one, and for some wavelengths, two significant figures. Since the results are reported as graphs, we felt that any higher accuracy would be superfluous.

and

$$C_0(x) = \cos(x), \quad C_1(x) = \frac{\cos(x)}{x} + \sin(x).$$

The derivatives of the Riccati-Bessel functions follow from the above definitions. Having found the Mie coefficients, the program then calculates the scattering functions for the perpendicular and plane polarized scattered waves, $i_1(\theta')$ and $i_2(\theta')$, as defined by equations 2.3 through 2.8. Recall (section 2.3) that the scattering angle θ' and the angle the detector makes with the z axis (the sun rays) θ are related by

$$\theta' = \pi - \theta.$$

The program then calculates, by use of equation 2.19, the ratio of the intensity of the scattered signal to the intensity of the incoming signal, $\frac{I}{I_0}$, for the view angle θ from 0 to 180 degrees. This corresponds to a scattering angle of 180 to 0 degrees. The program repeats the above process for all the divisions in the distribution.

In calculating the attenuation, we assumed that the signal travels the extent of the cloud. Thus, the attenuation has no angular dependence. However, the contributions of all the partitions must still be added, as indicated by equation 2.14. In addition, we found that the range of values in the attenuation, as given by equation 2.14, is very wide. Thus, we express it in terms of decibels:

$$\text{attenuation} = 10 \log \frac{I_0}{I},$$

or

$$\text{attenuation} = 4.343\gamma R_c.$$

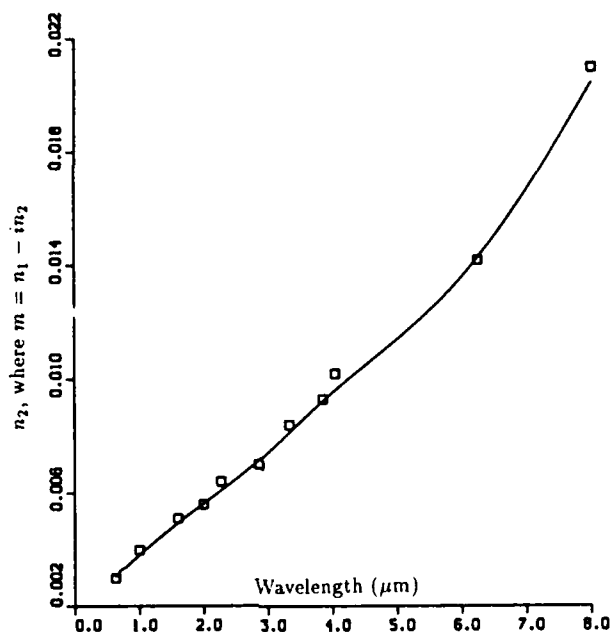


Figure 3.1: The imaginary part of the index of refraction for aluminum oxide at 2950 K [Bakhir 77].

To calculate the Mie coefficients, we need the value of the index of refraction of the substance at the frequency (and, thus, the wavelength) in question. We used the values calculated by Bakhir *et al.* [Bakhir 77], who published a graph of the dependence of the imaginary part of the index of refraction for aluminum oxide at 2950 K as a function of wavelength. We have reproduced their results in figure 3.1. They also published the dependence of the real part of the index of refraction on the wavelength in the form of a table. We reproduce this result in figure 3.2. For the index of refraction of smoke, we used $m = 1.75 - i0.45$, which was taken from Ramaswamy [Ramaswamy 85].

It was assumed that 1 kg of fuel was burned, and that the fraction of

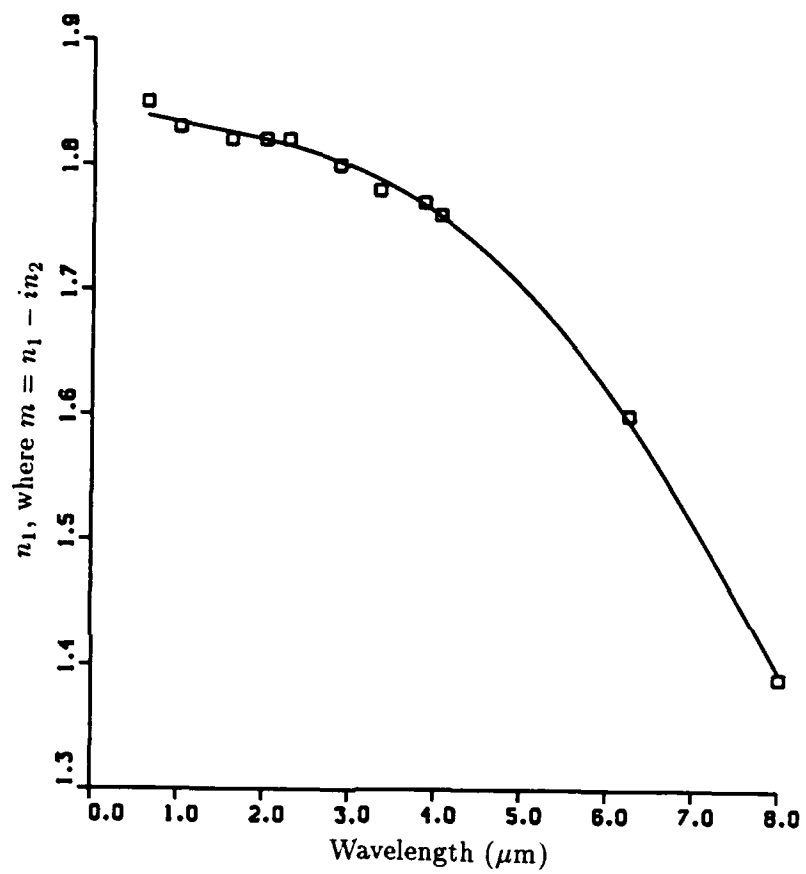


Figure 3.2: The real part of the index of refraction for aluminum oxide at 2950 K [Bakhr 77].

mass burned that turned into aluminum oxide or smoke particles is 0.05. The densities were taken as $2.0 \times 10^3 \text{ kg/m}^3$ for smoke and as $2.7 \times 10^3 \text{ kg/m}^3$ for aluminum oxide. The results are shown in the next section.

3.2 Results of the Models

The results are divided into two groups of graphs. The first group, figures 3.3 through 3.6, show the intensity (expressed as the ratio of the intensity reaching the detector and the initial intensity, $\frac{I}{I_0}$) of scattered light the detector receives. Each one of the graphs show the intensity as a function of the cloud extension (R_c in figure 2.3) and the detector's view angle for a given wavelength and index of refraction. For instance, figure 3.3 represents the ratio $\frac{I}{I_0}$ for the wavelength $\lambda = 4.04 \text{ } \mu\text{m}$ and index of refraction $m = 1.76 - i0.0102$ as a function of viewing angle for cloud extensions R_c of 1, 10, 100 and 1000 meters. The scattering particles are aluminum oxide in figures 3.3 through 3.5 and smoke in figure 3.6. It was assumed that the size distribution for the smoke particles was identical to the distribution of aluminum oxide. The information presented in these graphs may be used to determine the extent to which the scattered light masks the signal. Ultimately, the ability of the detector to distinguish the signal from the "noise" introduced by the scattered light will depend on the intensity of the incident light, I_0 , and the intensity of the signal itself, I_{signal} . While the intensity of sunlight is well known, a determination of the signal intensity and the detector's ability to distinguish the signal from the scattered "noise" is beyond the scope of this project.

The second group of results is shown in figure 3.7. This graph shows

the attenuation (as defined in section 3.1) of the signal itself as a function of extention R_c of the cloud. Since the attenuation in aluminum oxide for signals of wavelengths $4.04 \mu\text{m}$, $6.25 \mu\text{m}$ and $8.0 \mu\text{m}$ was found to be essentially identical, only the graph for $\lambda = 8.0 \mu\text{m}$ is shown. In addition, we also show, in the same graph, the attenuation of light at $\lambda = 10.0 \mu\text{m}$ for smoke. From this graph we see that the attenuation is in the order of 1db for a cloud extention of 10 meters, falling rapidly for greater cloud demensions. Thus, attenuation should not be a factor in the detection of signals for cloud extentions greater than 10 meters.

3.3 Conclusions

The results of the model for the scattered intensity, figures 3.3 through 3.6, show the ratio of scattered intensity to incident intensity $\frac{I}{I_0}$. This information can be used, in conjunction with information on the intensity of the sunlight and the signal itself, to determine the effect of the scattered light on the detector's ability to detect the signal. To calculate the graphs, we assumed that the amount of fuel burned is 1 kg, that the fraction of particles converted to aluminum oxide or smoke is 0.05, and that the densities are $2.7 \times 10^3 \text{ kg/m}^3$ for aluminum oxide and $2.0 \times 10^3 \text{ kg/m}^3$ for smoke.

The results for the attenuation are much easier to interpret. Figure 3.7 shows that the attenuation of a signal in the range of $10 \mu\text{m}$ is of the order of 1 db for a cloud of 10 m. The attenuation decreases rapidly with increasing cloud dimensions. Thus, the attenuation should not be a problem in signal detection once the cloud has dissipated to 10 meters or greater.

3.4 Recommendations for Further Work

Future investigations of this problem should look at the problem of a detector searching for a signal in a direction not in the plane defined by the cloud axis and the sun's rays. Although the theory of the problem is the same as in this presentation, the unusual geometry of an off-plane detector makes it much more complicated.

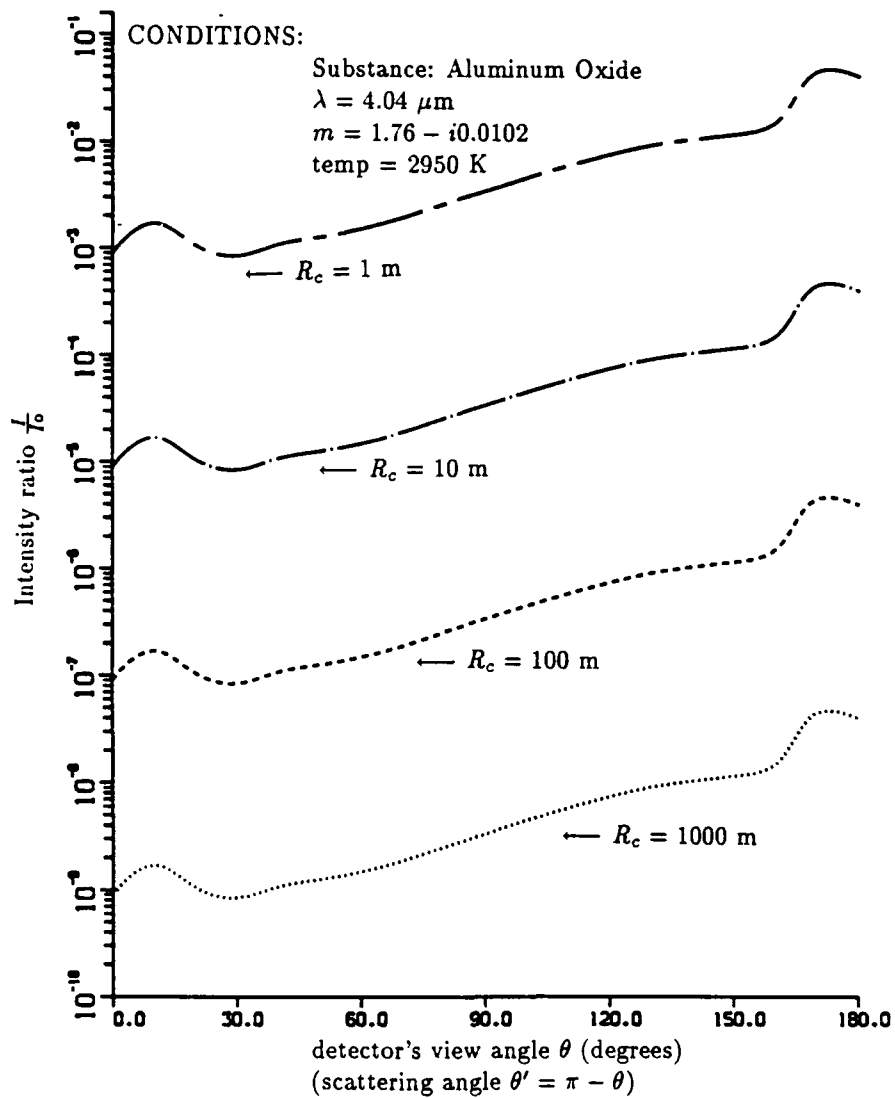


Figure 3.3: $\frac{I}{I_0}$ for the aluminum oxide particle distribution of a Titan-IIC rocket at $\lambda = 4.04 \mu\text{m}$.

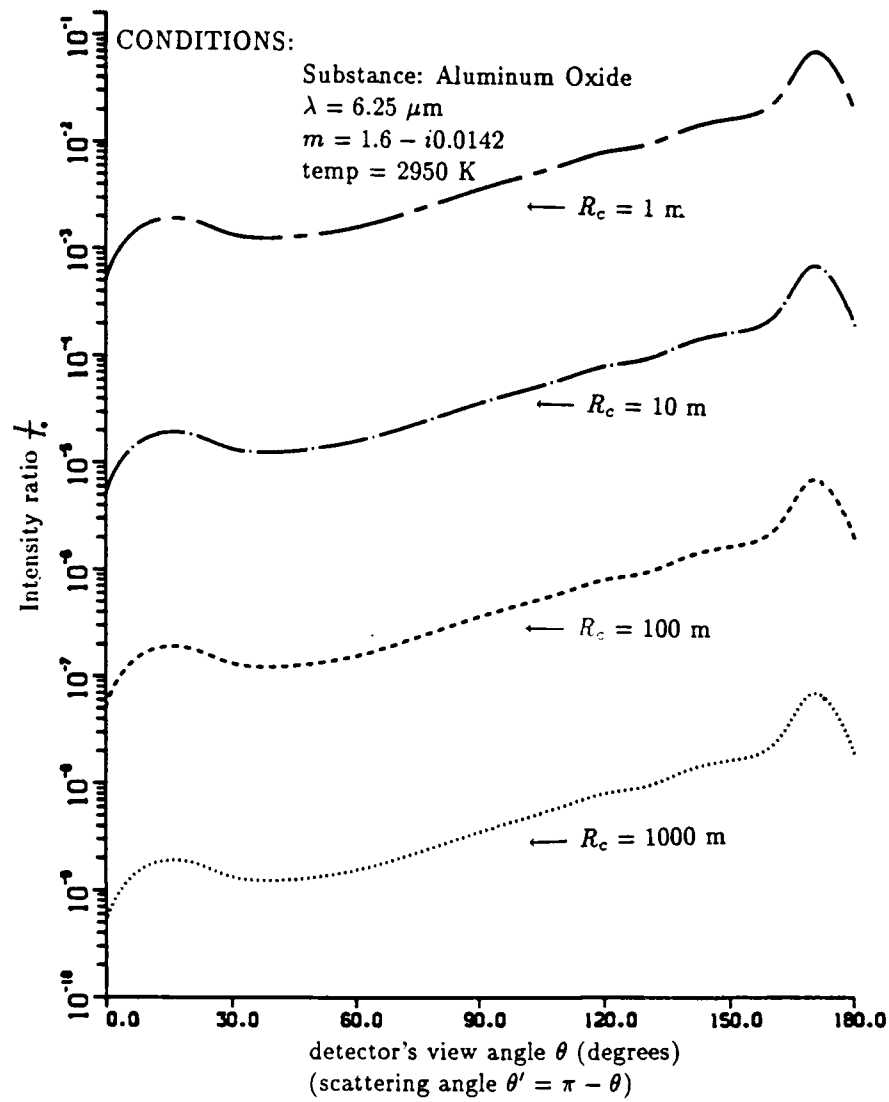


Figure 3.4: $\frac{I}{I_0}$ for the aluminum oxide particle distribution of a Titan-IIIC rocket at $\lambda = 6.25 \mu\text{m}$.

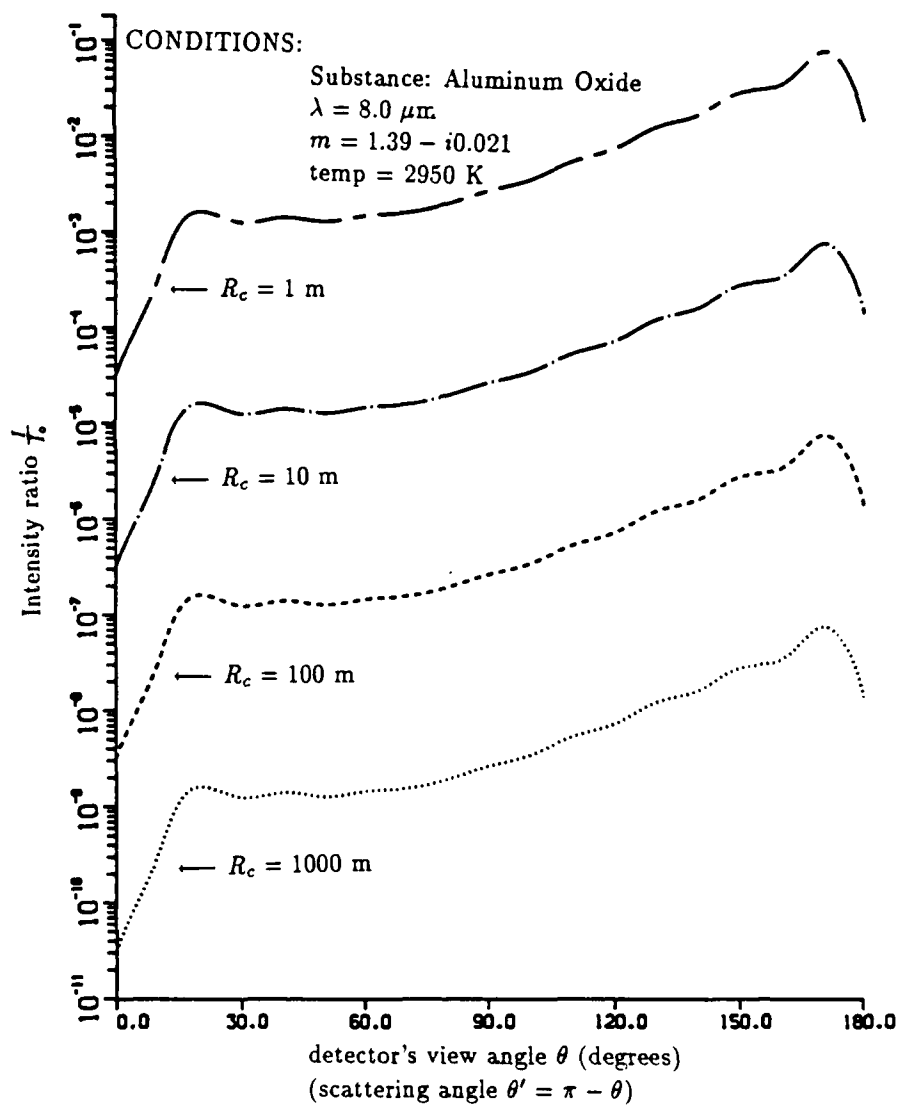


Figure 3.5: $\frac{I}{I_0}$ for the aluminum oxide particle distribution of a Titan-IIC rocket at $\lambda = 8.0 \mu\text{m}$.

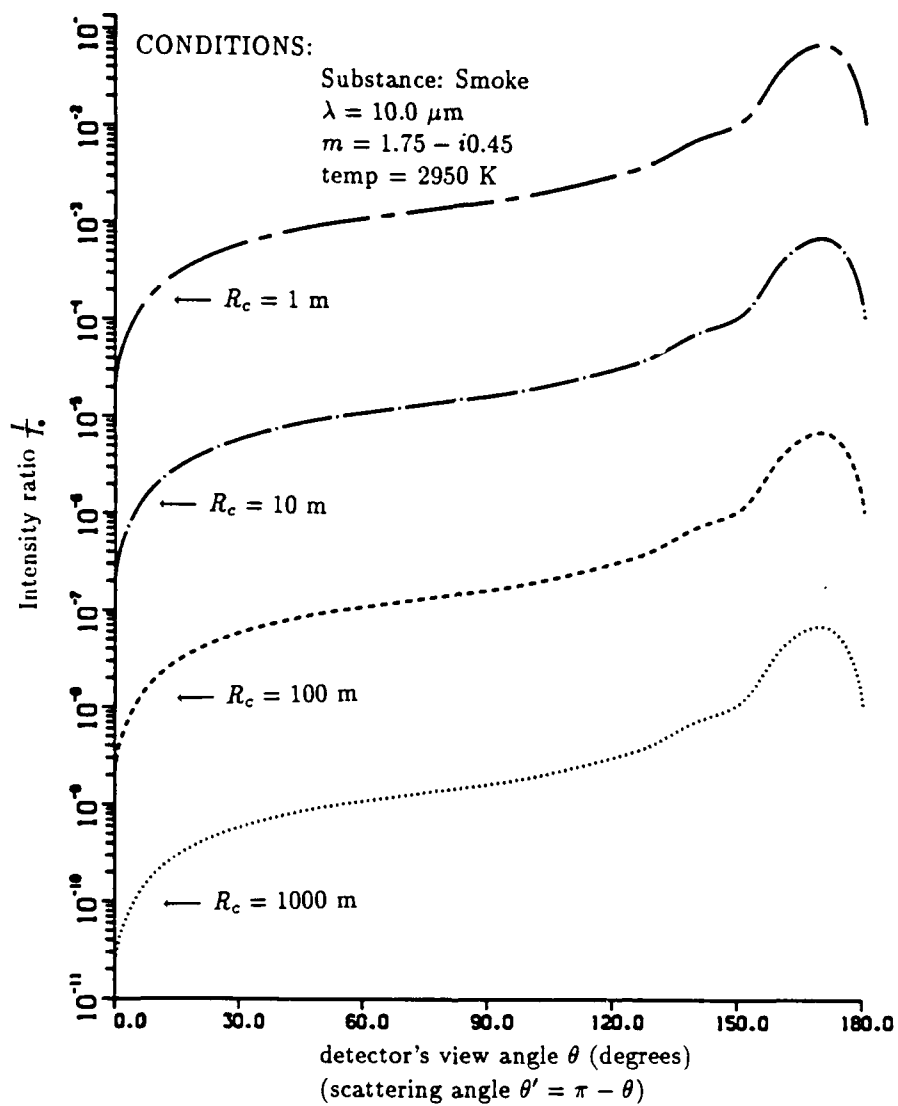


Figure 3.6: $\frac{I}{I_0}$ for the smoke particle distribution of a Titan-III rocket at $\lambda = 10.0 \mu\text{m}$.

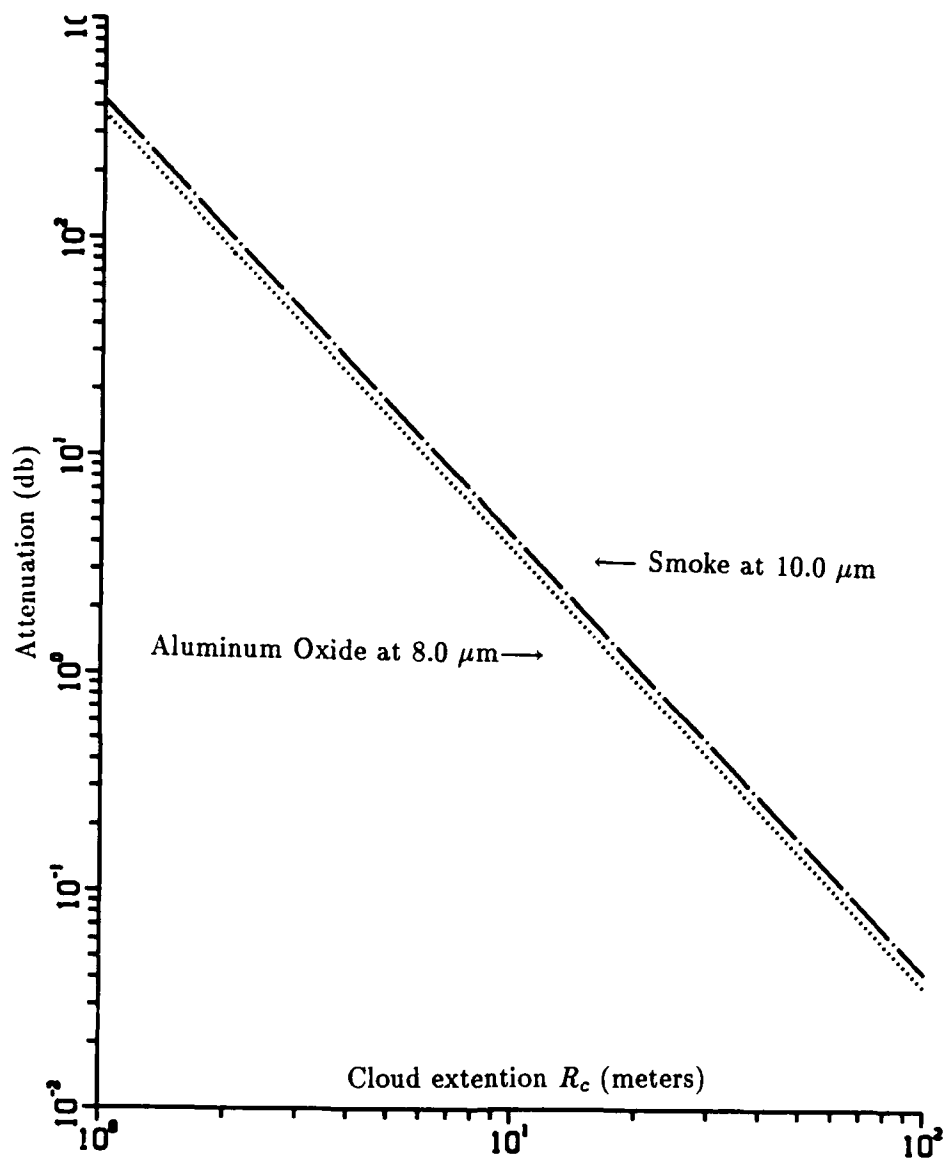


Figure 3.7: The attenuation for the aluminum oxide and smoke particle distribution of a Titan-IIIC rocket at $\lambda = 8.0 \mu\text{m}$ and $\lambda = 10.0 \mu\text{m}$, respectively.

Appendix A

The Computer Program

We have tried to make the program as self-explanatory and user-friendly as possible. Experience shows, however, that what is clear to the programmer need not be clear to the user. Thus, we include the following “pointers” in the hopes of clarifying the workings of the program.

- Whenever possible, the equations or formulas in the program are written in the form they are written in the text. Unfortunately, this is not always possible due to the limited selection of characters available to the programmer. For instance, while the text can easily handle characters such as λ and S_1 , the programmer does not have access to those characters. In those cases, we either spell the name of the variable (“lambda” for λ , for instance) or we try to associate a descriptive name with the variable (“numdivisions” for number of divisions.)
- The program asks the user to input the wavelength of the radiation, the number of partitions in the distribution, the extension of the cloud and the index of refraction. When supplying the data, it is extremely important that the data be in the units specified in the program; otherwise, although the program may run, the results will be meaningless (the program, as stands, does not check for the correct units nor dimensions.)

- In subroutines, the input and output arguments are separated in one of two fashions: by a space between the last input argument and the first output argument, or by placing the output arguments in a new line. Additionally, at the beginning of every subroutine, we say, in a comment box, which arguments are inputs and which are outputs.
- In addition to output arguments, subroutines may also create data files. These data files are then used by other subroutines.
- The results for the scattering problem ($\frac{I}{I_0}$) are stored in the file sums.dat, while the attenuation is stored in the file data file attenuation.dat.

Turn to the next page for the program.

program scattermain

```
*****
*Comment: Throughout the program, comments will be enclosed
*in boxes (such as this). This program asks the user to
*input the wavelength. For the program to run correctly,
*it should be expressed in micrometers (1E-06). On the other
*hand, the cloud radius should be in meters. It's very important
*to input the complex index of refraction as follows: if z is
*a complex number,  $z = a + ib$ , where a is the real part of z and
*b is the imaginary, then it should be typed as (a,b). Thus,
*z = 1.75 - i0.45 would be typed as (1.75,-0.45).
*
*NOTE: if data for a density, fraction of burned mass, or any
*other parameter, different from the ones used in the program,
*is wanted, then they must be changed in the declarations below
*****
```

```
double precision left,right,step,numberdensity(0:1000)
double precision Q(0:1000),totalgamma,gamma(0:1000)
double precision lambda,viewwidth,cloudradius,PI
double precision volume,k,intensity,sum(20),a,n
double precision density,massburned,cloudbase
complex refraction
integer i,numdivisions
```

```
external qamp,intensitysub
external particlepopulation
parameter (PI = 3.141592635)
parameter (viewwidth = 2.0)
parameter (massburned = 0.05)
parameter (left = 0.0)
parameter (right = 12.0)

open (1,file='viewwidth',status='new')
  write (1,*)viewwidth
close (1)

print *,'input density in kg/m(3)'
read *,density
print *,'input number of divisions (even)'
read *,numdivisions
print *,'input wavelenght in micrometers (10 (-6)m)'
read *,lambda
print *,'input cloudradius in meters'
read *,cloudradius
print *,'input the complex index of refraction
*   in this format: m = a+ib = (a,b)'
read *,refraction

k = (2.0*PI)/(lambda*1D-06)
```

```
*****
*the volume is different for different cloud shapes!!  If data
*for a cloud not in a cone shape is wanted (say, a sphere),
*then the following formula must be changed
*****
```

```
cloudbase = cloudradius/10.0
volume = (1.0/3.0)*PI*(cloudradius**2)*cloudbase
totalgamma = 0.0
```

```
step = (right - left)/numdivisions
```

```
call particlepopulation(numdivisions,left,step,volume,
*      massburned,density,PI)
```

```
open (1, file = 'population', status = 'old')
do 10, i = 0, (numdivisions -1),1
    read(1,*) numberdensity(i)
10  continue
close(1, status = 'delete')

do 09, i = 0, (numdivisions -1), 1
    n = (2*i + 1)/2.0
```

```
a = left + (n * step)
call qamp(a/lambda,refraction, Q(i))
gamma(i) = numberdensity(i)*PI*((a*1D-06)**2)*Q(i)
totalgamma = totalgamma + gamma(i)
call intensitysub(k,numberdensity,cloudradius)

open (1, file = 'intensity', status = 'old')
do 11, j=1, 19
    read (1,*)intensity
    sum(j) = sum(j) + intensity
11 continue
close (1, status = 'delete')
print*, 'this is division # / out of numdivisions:'
write(*,*)i,numdivisions
09 continue

open(1, file = 'totalgamma', status = 'new')
write(1,*)totalgamma
close(1)

*
* comment:  if needed, the total coefficient of extinction
* (totalgamma) may be obtained from the file totalgamma.dat
* above.
*
```



```
open (2, file = 'sums', status = 'new')
do 13, i = 1, 19
  write (2,*)sum(i)
13  continue
close (2)

open (1, file = 'attenuation',status = 'new')
  write (1,*)(4.343*totalgamma*cloudradius)
close(1)
end

*****
*Particlepopulation finds the actual number of particles
*as dictated by the distribution and the amount of fuel
*burned. It calls on the function "distribution."
*All the arguments are inputs. The output is the
*data file population.dat, which contains the normalized
*distribution of particles.
*****

subroutine particlepopulation(numdivisions,left,step,
* cloudvolume,massburned,density,PI)

integer numdivisions,i
```

```
double precision n,a,left,step,numnormalized(0:1000)
double precision particlevolume,denominator,numatrmax
double precision distribution,massburned,totalnum
double precision cloudvolume,numberdensity(0:1000),PI
double precision sumofparticles
double precision number(0:1000)
external distribution
```

```
sumofparticles = 0.0
do 9, i=0,(numdivisions-1),1
  n = (2*i +1)/2.0
  a = left + (n*step)
  number(i) = distribution(a,step)
  sumofparticles = sumofparticles + number(i)
  write(*,*)i,sumofparticles
```

```
9 continue
```

```
denominator = 0.0
do 10, i=0,(numdivisions-1),1
  n = (2*i +1)/2.0
  a = left + (n*step)
  numnormalized(i) = distribution(a,step)/sumofparticles
  particlevolume = 4.0/3.0 * PI * (a*1D-06)**3
  denominator = denominator + numnormalized(i)
```

```

*
*particlevolume
10  continue

numatrmx = massburned/(density*denominator)

do 11, i = 0, (numdivisions-1),1
  numberdensity(i) = numnormalized(i) * numatrmx
*
*
11  continue
                                     /cloudvolume

open (1, file = 'population', status = 'new')
do 12, i = 0, (numdivisions-1), 1
  write(1,*) numberdensity(i)
12  continue
close(1)

end
```

*Distribution finds the distribution of the particles.

*Called on by particlerepopulation. If a new distribution is

*to be studied, this is the place to insert that

*new distribution.

*Inputs: a (the radius of the particles), step (increment)

*Output: the value of the distribution at (a) times the step
 * (area under the curve)

```
double precision function distribution(a,step)
```

```
double precision a, step, distro, Diam
```

```
Diam = 2 * a
```

```
distro = (0.051 * (Diam)**2) *
```

```
* exp( (-1.89D-02)*((Diam)**2) )
```

```
distribution = distro * step
```

```
end
```

*The following subroutine is the most involved subroutine in the
 *program. It may be considered the heart of the program.

*For a given size of particles, it calculates the Riccati-Bessel

*functions needed to find the Mie coefficients. Finds the

*coefficient of extinction, QEXT.

*Inputs: x = a/lambda (particle radius/wavelength)

* m = index of refraction

*Outputs: coefficient of extinction, QEXT, mie coefficients

*a and b in the file aandb.dat

*Calls on subroutine amplitude, which calculates i1 and i2

SUBROUTINE QAMP(X,M, QEXT)

COMPLEX M, SY(0:50), SYP(0:50), Y, ZETA(0:50)

COMPLEX ZETAP(0:50), A(50), B(50)

DOUBLE PRECISION LAMBDA, PI, X, SX(0:50), SXP(0:50)

DOUBLE PRECISION SUMQSCA, QSCA, OLDQSCA, XOFTHETA, THETA

DOUBLE PRECISION CX(0:50), CXP(0:50), QEXT, OLDQEXT

DOUBLE PRECISION SUMQEXT, TOLERANCE

INTEGER N, MAXITS, LIMIT

INTRINSIC SIN, COS, ABS

PARAMETER (PI = 3.1415926356)

PARAMETER (LIMIT = 50)

PARAMETER (TOLERANCE = 0.00001)

EXTERNAL INITIALRICCATI, INITIALRICCATI1

EXTERNAL QEXTING, DERIVATIVES, AANDB

EXTERNAL QSCATT,AMPLITUDE, RICCATIBESSEL

X = 2*PI*X

Y = M*X

SUMQEXT = 0

SUMQSCA = 0

QEXT = 0

QSCA = 0

MAXITS = 10

CALL INITIALRICCATI(X, Y,

* CX(0), SX(0), SY(0), ZETA(0),

* CXP(0), SXP(0), SYP(0), ZETAP(0))

*Comment: the above routine sets up the initial Riccati-Bessel

* function and its derivative.

N = 1

CALL INITIALRICCATI1(X,Y, CX(1),SX(1),SY(1),ZETA(1))

CALL DERIVATIVES(SX(N-1),SX(N),CX(N-1),CX(N),SY(N-1),

* SY(N),N,X,Y, CXP(N),SXP(N),SYP(N),ZETAP(N))

1492 DO 10, N = 2, MAXITS

CALL RICCATIBESSEL(N,X,Y,SX(N-1),SX(N-2),CX(N-1),

* CX(N-2),SY(N-1),SY(N-2),

* CX(N),SX(N),SY(N),ZETA(N))

CALL DERIVATIVES(SX(N-1),SX(N),CX(N-1),CX(N),SY(N-1),

```

*          SY(N),N,X,Y,  CXP(N),SXP(N),SYP(N),ZETAP(N))
10  CONTINUE

      DO 11, N = 1, MAXITS
      CALL AANDB(SX(N),SXP(N),SY(N),SYP(N),ZETA(N),
*          ZETAP(N),M,  A(N),B(N))
11  CONTINUE

      DO 12, N = 1, MAXITS
      OLDQEXT = QEXT
      CALL QEXTING(A(N), B(N), SUMQEXT, X, N,
*          QEXT, SUMQEXT)
      IF ((ABS(QEXT - OLDQEXT)).LE.(TOLERANCE)) THEN
          GO TO 13
      END IF
12  CONTINUE

      IF (MAXITS.EQ.LIMIT) THEN
          GO TO 21
      END IF

*COMMENT:  If MAXITS has not reached the limit, then increment
*          by 10 and go through the process again.
```

```
MAXITS = MAXITS + 10
GO TO 1492

21  WRITE(*,2000)QEXT
    GO TO 14

13  WRITE(*,2010)QEXT

14  OPEN (3,FILE = 'AANDB', STATUS = 'NEW')
    DO 20, N = 1, MAXITS
    WRITE (3,*) REAL(A(N)), AIMAG(A(N)),
*           REAL(B(N)), AIMAG(B(N))
20  CONTINUE
    CLOSE (3)

    CALL AMPLITUDE(MAXITS)

2000 FORMAT(1X,'Qext not converged after LIMIT number of
* terms. So far, Qext = ',E12.4)
2010 FORMAT(1X,'Qext converged to ',E12.4)

END
```

* Subroutines for QAMP follow

* Most of the 'set up' subroutines are self-explanatory.

* For instance, the subroutine initialriccati finds the

* initial values for the riccati-bessel functions, while the

* subroutine derivatives finds the derivatives of the

* riccati-bessel functions.

SUBROUTINE INITIALRICCATI(X,Y,

* CX, SX, SY, ZETA,

* CXP, SXP, SYP, ZETAP)

INTRINSIC SIN, COS

REAL X, CX, SX, CXP, SXP

COMPLEX Y, SY, ZETA

COMPLEX SYP, ZETAP

SX = SIN(X)

CX = COS(X)

SY = SIN(Y)

ZETA = CMLX(SX,CX)


```

REAL X, SXNM, SXNMM, CXNM, CXNMM, CXN, SXN
COMPLEX ZETAN, Y, SYN, SYNM, SYNMM
INTEGER N

```

```

SXN = ((2*N-1)/X)*SXNM - SXNMM
CXN = ((2*N-1)/X)*CXNM - CXNMM
SYN = ((2*N-1)/Y)*SYNM - SYNMM
ZETAN = CMLX(SXN, CXN)

```

```

END

```

```

SUBROUTINE AANDB(SX, SXP, SY, SYP, ZETA, ZETAP, MM,
*              A, B)

```

```

REAL    SX, SXP
COMPLEX SY, SYP, ZETA, ZETAP, MM, A, B

```

```

A = (SYP*SX - MM*SY*SXP)/(SYP*ZETA - MM*SY*ZETAP)
B = (MM*SYP*SX - SY*SXP)/(MM*SYP*ZETA - SY*ZETAP)

```

```

END

```

```

SUBROUTINE QEXTING(A, B, TEMPSUM, XTEMP, NTEMP,
*              QTEMP, TSUM)

```

```
REAL          TSUM, TEMPSUM, QTEMP, XTEMP
COMPLEX       A, B
INTEGER       NTEMP
```

```
TSUM = ((2*NTEMP + 1)*REAL(A + B)) + TEMPSUM
QTEMP = (2/XTEMP**2)*TSUM
```

```
END
```

```
SUBROUTINE QSCATT(A, B, TEMPSUM, X, N,
*              QSCA, SUM)
```

```
REAL          TEMPSUM, SUM, QSCA, X
COMPLEX       A, B
INTEGER       N
```

```
SUM = (2*N + 1) * ((ABS(A))**2 + (ABS(B))**2) + TEMPSUM
QSCA = (2/X**2)*SUM
```

```
END
```

```
SUBROUTINE DERIVATIVES(SXNM, SXN, CXNM, CXN, SYNM, SYN,
```

```
*           N, X, Y,   CXPB, SXPB, SYPB, ZETAPB)
```

```
REAL           SXNB, SXB, CXNB, CXB, X, CXPB, SXPB
```

```
COMPLEX        ZETAPB, SYNB, SYB, SYPB, Y
```

```
INTEGER        N
```

```
SXPB = SXNB - (N/X)*SXB
```

```
CXPB = CXNB - (N/X)*CXB
```

```
SYPB = SYNB - (N/Y)*SYB
```

```
ZETAPB = COMPLEX(SXPB,CXPB)
```

```
END
```

```
*****
```

```
* Comment: Subroutine amplitude finds the scattering functions
```

```
* for the perpendicular and plane polarized scattered waves,
```

```
* i1 and i2, respectively.
```

```
* Inputs: maxits. Also uses the data files aandb.dat and
```

```
* viewwidth.dat
```

```
* Output: i1 and i2 in the data file i1andi2.dat
```

```
*****
```

```
SUBROUTINE AMPLITUDE(MAXITS)
```

```
complex a(0:50),b(0:50),sone,stwo,oldsone,oldstwo
```

```
complex temp
```

```
double precision pprime(0:50),pdoubleprime(0:50)
double precision tau(0:50), p(0:50), viewwidth
double precision tolerance,reala,imaga,realb,imagb
double precision i1(0:1,0:18),i2(0:1,0:18),PI,theta,x
double precision viewby2,angledegrees, angleradians
double precision sine(0:1,0:18)
integer n,maxits,count,side
parameter (tolerance = 0.01)
parameter (PI = 3.141592654)
intrinsic COS, CMPLX,abs,SIN
```

```
open (1,file='viewwidth',status='old')
  read (1,*)viewwidth
close(1)
```

```
open(1,file='aandb',status='old')
do 13, n = 1, maxits
  read(1,*,end = 14)reala,imaga,realb,imagb
  a(n) = CMPLX(reala,imaga)
  b(n) = CMPLX(realb,imagb)
```

```
13 continue
```

```
14 close(1, status = 'delete')
```

```
open(2, file = 'i1andi2', status = 'new')
```

```
viewby2 = viewwidth/2.0
```

```
count = -1
```

```
do 1990, theta = 0, 180, 10
```

```
count = count + 1
```

```
do 09, side = 0, 1, 1
```

```
angledegrees = theta - viewby2 + (viewby2 * side * 2)
```

```
angleradians = angledegrees * PI/180.0
```

```
x = COS(PI - angleradians)
```

```
p(0) = 1
```

```
p(1) = x
```

```
do 10, n = 2, maxits
```

```
  p(n) = 2*x*p(n-1) - p(n-2) - (x*p(n-1) - p(n-2))/n
```

```
10  continue
```

```
pprime(0) = 0
```

```
pprime(1) = 1
```

```
do 11, n = 2, maxits
```

```
  pprime(n) = n*p(n-1) + x*pprime(n-1)
```

```
11  continue
```

```
pdoubleprime(0) = 0
```

```
pdoubleprime(1) = 0
```

```
do 111, n = 2, maxits
```

```

      pdoubleprime(n) = (2*n - 1)*pprime(n-1) +
*
*                                     pdoubleprime(n-2)
111  continue

      do 12, n = 0, maxits
      tau(n) = x*pprime(n) - (1-x**2)*pdoubleprime(n)
12   continue

      sone = cmplx(0.0,0.0)
      do 15, n = 1, maxits
      oldsone = sone
      temp = a(n)*pprime(n) + b(n)*tau(n)
      sone = ( temp * (2*n + 1)/(n*(n+1)) ) + oldsone
      if ((abs(sone - oldsone)).le.(tolerance)) then
      go to 16
      end if
15   continue

      print*, 'WARNING: S1 (and i1) not converged'
16   i1(side,count) = (abs(sone))**2

      stwo = cmplx(0.0,0.0)
      do 18, n = 1, maxits
      oldstwo = stwo
      temp = b(n)*pprime(n) + a(n)*tau(n)
```



```
      stwo = ( temp * (2*n +1)/(n*(n+1)) ) + oldstwo
      if ((abs(stwo - oldstwo)).le.(tolerance)) then
        go to 19
      end if
18      continue

      print *, 'WARNING: S2 (and i2) not converged'
19      i2(side,count) = (abs(stwo))**2

      sine(side,count) = ABS(SIN(angleradians))

09      continue

      write(2,*)i1(0,count),i2(0,count),sine(0,count),
*           i1(1,count),i2(1,count),sine(1,count)

1990     continue
        close(2)

      end

*****
*The above subroutine was the last subroutine in QAMP.  By now,*
*the program has calculated, for a given particle radius,
*the extinction coefficient, gamma, the amplitudes i1 and i2. *
```

*The following subroutine uses i1 and i2 to find the total
 *intensity of the scattered light reaching the sensor. This
 *total intensity is the integral of the intensity over the
 *solid angle the viewer "sees." The integration is accomplished
 *numerically (of course), in this subroutine.

*Input: k, numberdensity, cloudradius

*Output: the intensity of scattered light for one particular

* direction in the data file intensity.dat

```
subroutine intensitysub(k,numberdensity,cloudradius)
```

```
integer count,side
```

```
double precision i1(0:1,0:18),i2(0:1,0:18)
```

```
double precision sine(0:1,0:18), numberdensity
```

```
double precision foftheta(0:1), integral, viewby2, PI
```

```
double precision intensity(0:18),viewwidth,k
```

```
double precision cloudradius,geomfactor
```

```
parameter (PI = 3.1415926356)
```

```
open (1,file = 'viewwidth',status = 'old')
```

```
read (1,*)viewwidth
```

```
close (1)
```

```
open (1,file = 'i1andi2', status = 'old')
```

```

do 10, count = 0, 18
  read (1,*)i1(0,count),i2(0,count),sine(0,count),
*      i1(1,count),i2(1,count),sine(1,count)
10  continue
    close (1, status = 'delete')

viewby2 = viewwidth/2.0

*****
*The geometric factor depends only on the solid angle that
*the detector "sees." Thus, it is independent of the sshape
*of the cloud, as long as the detector's field of view lies
*completely within the cloud
*****

geomfactor = (numberdensity*PI*cloudradius)/(k**2)

do 11, count = 0, 18
  do 12, side = 0, 1
    foftheta(side)=sine(side,count)*( i1(side,count) +
*                                     i2(side,count) )
12  continue

integral = ( foftheta(0) + foftheta(1) ) *
*          ( viewby2 * PI / 180.0)

```

```
intensity(count) = geomfactor * integral
```

```
11 continue
```

```
open (2,file = 'intensity', status = 'new')
```

```
do 13, count = 0, 18
```

```
write (2,*)(intensity(count))
```

```
13 continue
```

```
close(2)
```

```
end
```

BIBLIOGRAPHY

- [Arfken 85] Arfken, G., *Mathematical Methods for Physicists*, 3rd ed. San Diego: Academic Press, Inc. (1985).
- [Bakhrir 77] Bakhrir, L. P., G. I. Levanshenko and V. V. Tamarovich, *J. Appl. Spectrosc.*, **26**, 378 (1977).
- [Dawbarn 80] Dawbarn, R., M. Kinslow and D. J. Watson, *Analysis of the Measured Effects of the Principal Exhaust Effluents From Solid Rocket Motors*. NASA contractor report 3136. NASA Scientific and Technical Information Office (1980).
- [Griffiths 81] Griffiths, D. J., *Introduction to Electrodynamics*. Englewood Cliffs: Prentice-Hall, Inc. (1981).
- [Gumprecht 51] Gumprecht, R. O. and C. M. Sliepcevich, *Tables of Riccati-Bessel Functions for Large Arguments and Orders*. Ann Arbor: Edwards Brothers, Inc. (1951)
- [Jackson 75] Jackson, J. D., *Classical Electrodynamics*, 2nd ed. New York: John Wiley & Sons (1975).
- [Mie 08] Mie, G., *Ann. Physik*, **25**, 377 (1908).
- [Mularz 72] Mularz, E. J. and M. C. Yuen, *J. Quant. Spectros. Radiat. Transfer*, **12**, 1553 (1972).

- [Ramaswamy 85] Ramaswamy, V. and J. T. Kiehl, *J. Geophys. Resear.*, **90**, 5597 (1985).
- [Slater 47] Slater, J. C. and N. H. Frank, *Electromagnetism*. New York: McGraw-Hill Book Company, Inc. (1947).
- [van de Hulst 81] van de Hulst, H. C., *Light Scattering by Small Particles*. New York: Dover Publications, Inc. (1981).

VITA

Jose Mario Pauda [REDACTED]

[REDACTED]. At the age of six, he moved with his parents, Julian Octavio Pauda and Maria Pauda, to Durango, Mexico, where he completed his elementary education. Upon returning to the United States, he graduated from San Jose High School in 1976 and then attended the University of California at Santa Barbara for two years. He transferred to the Air Force Academy in 1978, where he earned a Bachelor of Science in Physics degree and received a commission in the United States Air Force on June 2, 1982. He completed pilot training in 1983 and the B-52 Combat Crew Training Course in 1984. He served as copilot and aircraft commander of B-52G's and B-52H's at Fairchild AFB, Washington, until August, 1988, when he reported to the University of Texas at Austin to pursue his master's degree in physics. He lives with his wife of six years, [REDACTED], and their 19-month old son, [REDACTED].

[REDACTED] Dr.
[REDACTED]
[REDACTED]

¹ L^AT_EX document preparation system was developed by Leslie Lamport as a special version of Donald Knuth's T_EX program for computer typesetting. T_EX is a trademark of the American Mathematical Society. The L^AT_EX macro package for The University of Texas at Austin thesis format was written by Khe-Sing The.